Available online at www.sciencedirect.com

SciVerse ScienceDirect

Ceramics International 38 (2012) 4953–4959

CERAMICS INTERNATIONAL

www.elsevier.com/locate/ceramint

Electrochemical properties of $LiNi_{1-y}Co_yO_2$ ($y = 0.1$, 0.3 and 0.5) synthesized from $LiOH{\cdot}H_2O$, NiO and Co_3O_4 by solid state reaction method

Myoung Youp Song [a,*], Eui Yong Bang [b], Daniel R. Mumm [c], Hye Ryoung Park [d]

[a] Division of Advanced Materials Engineering, Department of Hydrogen and Fuel Cells, Hydrogen & Fuel Cell Research Center, Engineering Research Institute, Chonbuk National University, 567 Baekje-daero Deokjin-gu Jeonju, 561-756, Republic of Korea

[b] Hanwha Chemical Research & Development Center, 6 Shinseong-Dong Yuseong-Gu Daejeon, 305-804, Republic of Korea

[c] Department of Chemical Engineering and Materials Science, University of California Irvine, Irvine, CA, 92697-2575, USA

[d] School of Applied Chemical Engineering, Chonnam National University, 300 Yongbong-Dong Buk-Gu Gwangju, 500-757, Republic of Korea

Received 19 January 2012; received in revised form 20 February 2012; accepted 25 February 2012
Available online 5 March 2012

Abstract

$LiNi_{1-y}Co_yO_2$ ($y = 0.1$, 0.3 and 0.5) were synthesized by solid state reaction method at 750 °C and 850 °C from $LiOH{\cdot}H_2O$, NiO and Co_3O_4 as starting materials. The electrochemical properties of the synthesized $LiNi_{1-y}Co_yO_2$ were investigated. The synthesized $LiNi_{1-y}Co_yO_2$ had a α-$NaFeO_2$ structure with a space group of $R\bar{3}m$. Among all of the prepared $LiNi_{1-y}Co_yO_2$ ($y = 0.1$, 0.3 and 0.5) samples, $LiNi_{0.7}Co_{0.3}O_2$ calcined at 850 °C for 40 h had the largest first discharge capacity of 146.2 mAh/g and a relatively low discharge capacity fading rate.

Keywords: $LiNi_{1-y}Co_yO_2$; Solid state reaction method; Degree of displacement of the nickel and lithium ions; Discharge capacity; Capacity fading rate

1. Introduction

Many researchers have investigated transition metal oxides such as $LiCoO_2$ [1–5], $LiNiO_2$ [6–15], and $LiMn_2O_4$ [16–22] as cathode materials for lithium secondary batteries [23]. $LiMn_2O_4$ is relatively cheap and does not cause environmental pollution, but its cycling performance is poor. $LiCoO_2$ has a large diffusivity and a high operating voltage, and it can be easily prepared. However, it has a disadvantage that it contains an expensive element, Co.

$LiNiO_2$ is a very promising cathode material since it has a large discharge capacity [24] and is relatively excellent from the viewpoints of economics and environment. However, due to the similar sizes of Li and Ni ($Li^+ = 0.72$ Å and $Ni^{2+} = 0.69$ Å), the $LiNiO_2$ is practically obtained in the non-stoichiometric compositions, $Li_{1-y}Ni_{1+y}O_2$ [25,26], and the Ni^{2+} ions in the lithium planes obstruct the movement of the Li+ ions during charge and discharge [27,28].

The drawbacks of $LiCoO_2$ and $LiNiO_2$ can be overcome by incorporating phases with $LiNi_{1-y}Co_yO_2$ compositions because the presence of cobalt stabilizes the structure in a strictly two-dimensional fashion, thus favoring good reversibility of the intercalation and deintercalation reactions [27,29–42]. Rougier et al. [27] reported that the stabilization of the two-dimensional character of the structure by cobalt substitution in $LiNiO_2$ is correlated with an increase in the cell performance, due to the decrease in the amount of extra-nickel ions in the inter-slab space which impede the lithium diffusion. Kang et al. [42] investigated the structure and electrochemical properties of the Li_xCo_y-$Ni_{1-y}O_2$ ($y = 0.1$, 0.3, 0.5, 0.7, 1.0) system synthesized by solid state reaction with various starting materials to optimize the characteristics and synthetic conditions of the $Li_xCo_yNi_{1-y}O_2$. The first discharge capacities of $Li_xCo_yNi_{1-y}O_2$ were 60–180 mAh/g depending on synthetic conditions.

In this work, $LiNi_{1-y}Co_yO_2$ ($y = 0.1$, 0.3 and 0.5) cathode materials were synthesized by solid state reaction method at different temperatures using $LiOH{\cdot}H_2O$, NiO and Co_3O_4 as starting materials. The electrochemical properties of the synthesized samples were then investigated.

2. Experimental

$LiOH{\cdot}H_2O$ (High Purity Chemical Laboratory Co., purity 99%), NiO (High Purity Chemical Laboratory Co., purity

* Corresponding author. Tel.: +82 63 270 2379; fax: +82 63 270 2386.
E-mail address: songmy@jbnu.ac.kr (M.Y. Song).

0272-8842/$36.00
doi:10.1016/j.ceramint.2012.02.089

99.9%) and Co_3O_4 (High Purity Chemical Laboratory Co., purity 99.9%) were used as starting materials in order to synthesize $LiNi_{1-y}Co_yO_2$ by the solid-state reaction method.

The experimental procedure is shown schematically in Fig. 1. Starting materials with the compositions of $LiNi_{1-y}Co_yO_2$ ($y = 0.1$, 0.3 and 0.5) were mixed and pelletized. These pellets were heat-treated in air at 650 °C for 20 h, and were ground, mixed, and pelletized again. They were then calcined at 750 °C or 850 °C for 20 h. Pellets were cooled at a cooling rate of 50 °C/min, ground, mixed and pelletized again. They were then calcined again at 750 °C or 850 °C for 20 h.

Phase identification of the synthesized samples was carried out by X-ray diffraction (XRD) analysis with Cu K_α radiation using a Rigaku type III/A X-ray diffractometer. The scanning rate was 4°/min and the scanning range of the diffraction angle (2θ) was $10^\circ \leq 2\theta \leq 70^\circ$. The morphologies of the samples were observed using a field emission scanning electron microscope (FE-SEM). The particle size distributions and the specific surface areas of the samples were analyzed by a particle size analyzer (Malvern Instruments).

The electrochemical cells consisted of $LiNi_{1-y}Co_yO_2$ as a cathode, Li foil as an anode, and an electrolyte (Purelyte, Samsung Chemicals Ltd.) prepared by dissolving 1 M $LiPF_6$ in a 1:1 (volume ratio) mixture of ethylene carbonate (EC) and dimethyl carbonate (DMC). A Whatman glass-fiber was used as the separator. To fabricate the cathode, 89 wt.% synthesized $LiNi_{1-y}Co_yO_2$, 10 wt.% acetylene black and 1 wt.% polytetrafluoroethylene (PTFE) binder were mixed in an agate mortar. The cell was assembled in a glove box filled with argon. All of the electrochemical tests were performed at room temperature with a potentiostatic/galvanostatic system. The cells were cycled at a current density of 200 $\mu A/cm^2$ between 3.2 and 4.3 V.

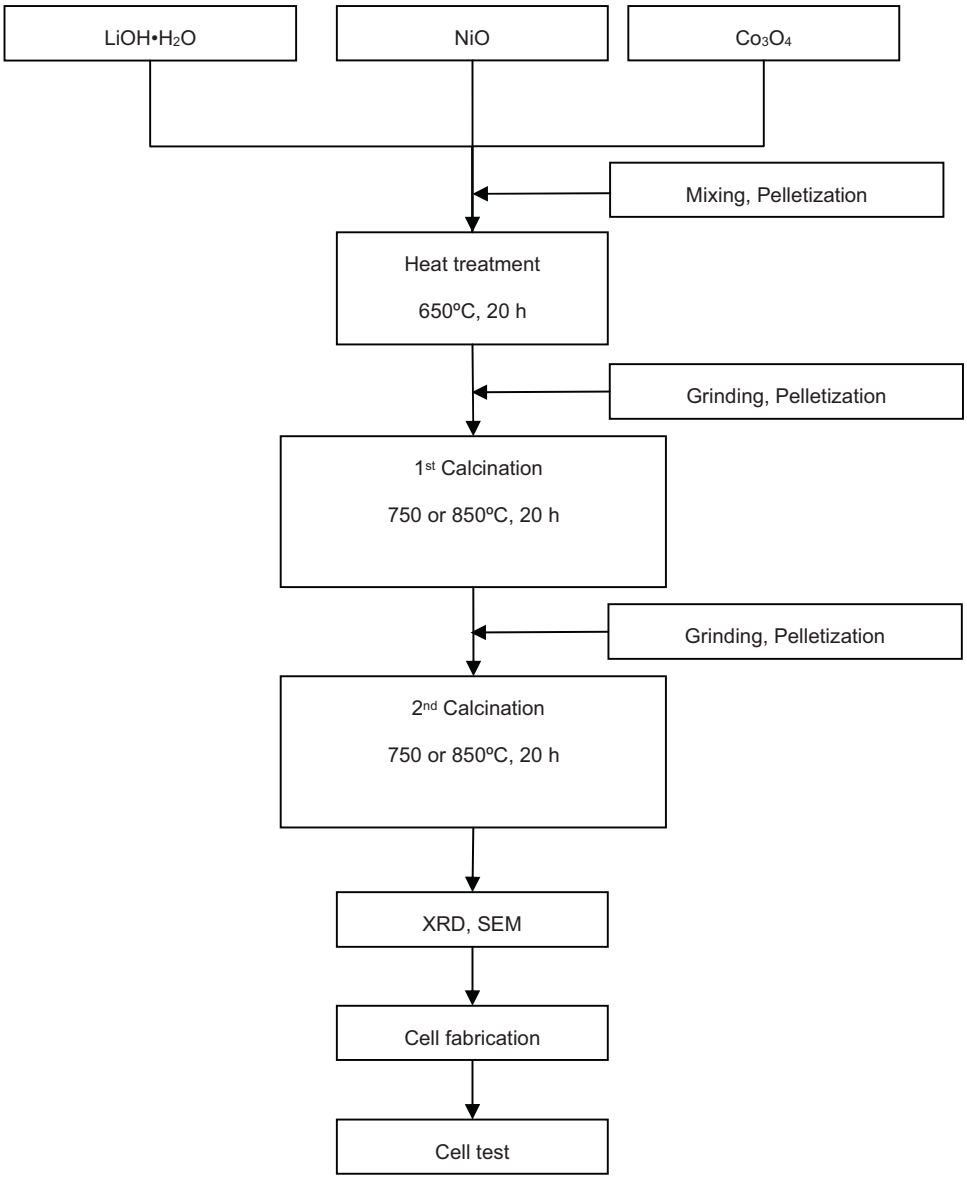

Fig. 1. Experimental procedure to synthesized $LiNi_{1-y}Co_yO_2$ ($y = 0.1$, 0.3 and 0.5) by the solid state reaction method from $LiOH{\cdot}H_2O$, NiO and Co_3O_4.

3. Results and discussion

Fig. 2 shows the XRD patterns of $LiNi_{1-y}Co_yO_2$ ($y = 0.1$, 0.3 and 0.5) powders calcined at 750 °C for 40 h from $LiOH{\cdot}H_2O$, NiO and Co_3O_4. They were identified as corresponding to a α-$NaFeO_2$ structure with a space group of $R\bar{3}m$. Impurity peaks appear at diffraction angles $2\theta = 21^\circ$ and 32°. These peaks were identified as those of the Li_2CO_3 phase. As the Co content increases, the intensities of these peaks decrease. Ohzuku et al. [43] reported that electroactive $LiNiO_2$ showed a clear split of the (1 0 8) and (1 1 0) lines, which appear in their XRD patterns at the diffraction angle near $2\theta = 65^\circ$ around. The splitting of the (1 0 8) and (1 1 0) lines in Fig. 2 becomes more distinct as the Co content increases.

XRD patterns of $LiNi_{1-y}Co_yO_2$ ($y = 0.1$, 0.3 and 0.5) powders calcined at 850 °C for 40 h from $LiOH{\cdot}H_2O$, NiO and Co_3O_4 are exhibited in Fig. 3. They also have the phase with the α-$NaFeO_2$ structure with a space group of $R\bar{3}m$. As the Co content increases, the intensities of the peaks of Li_2CO_3 phase appearing at diffraction angles $2\theta = 21^\circ$ and 32° decrease quite rapidly, and they do not appear in the $LiNi_{0.5}Co_{0.5}O_2$ sample. The peaks of Li_2CO_3 phase become weaker, compared with those in Fig. 2. The splitting of the (1 0 8) and (1 1 0) lines becomes more distinct as the Co content increases. The splittings of the (1 0 8) and (1 1 0) lines of $LiNi_{1-y}Co_yO_2$ ($y = 0.1$, 0.3 and 0.5) calcined at 850 °C (Fig. 3) are more distinct than those of $LiNi_{1-y}Co_yO_2$ ($y = 0.1$, 0.3 and 0.5) calcined at 750 °C (Fig. 2).

The 0 0 3 peak originates from the diffraction of only the $R\bar{3}m$ α-$NaFeO_2$ structure, while the 1 0 4 peak originates from the diffractions of both the $R\bar{3}m$ α-$NaFeO_2$ and $Rm\bar{3}m$ NaCl structures. Therefore, it is possible to calculate the fraction of each phase from the intensity ratio of the 0 0 3 and 1 0 4 peaks. Morales et al. [44] reported that the intensity ratio, $I_{0\,0\,3}/I_{1\,0\,4}$, of the completely stoichiometric composition $LiNiO_2$ is about 1.3. Ohzuku et al. [43] investigated the factors affecting the

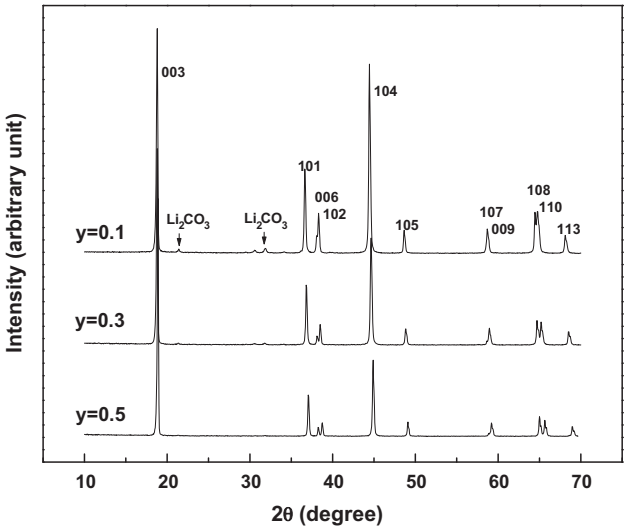

Fig. 3. XRD patterns of $LiNi_{1-y}Co_yO_2$ ($y = 0.1$. 0.3 and 0.5) powders calcined at 850 °C for 40 h from $LiOH{\cdot}H_2O$, NiO and Co_3O_4.

electrochemical reactivity of $LiNiO_2$. They reported that the intensity ratio of the 0 0 3 and 1 0 4 peaks is a key parameter of the degree of displacement of the nickel and lithium ions. As the intensity ratio of the 0 0 3 and 1 0 4 peaks increases, the degree of displacement of the nickel and lithium ions decreases. The disordered region prevents the extension and reduction of the interlayer distance between the NiO_2 sheets, making sliding between the basal planes impossible. Consequently, the nickel ions in the lithium sheet including the near neighbors are inactive for the electrochemical reaction. This is the reason that the samples having a high concentration of nickel ions at the lithium sites are inactive in nonaqueous lithium cells.

The variation of intensity ratio of 0 0 3 and 1 0 4 peaks, $I_{0\,0\,3}/I_{1\,0\,4}$, with y in $LiNi_{1-y}Co_yO_2$ calcined at 750 °C and 850 °C for 40 h is presented in Fig. 4. As the value of y increases, the value of $I_{0\,0\,3}/I_{1\,0\,4}$ for $LiNi_{1-y}Co_yO_2$ calcined at 850 °C increases rapidly, and that for $LiNi_{1-y}Co_yO_2$ calcined at 750 °C increases slowly. This shows that as the calcination

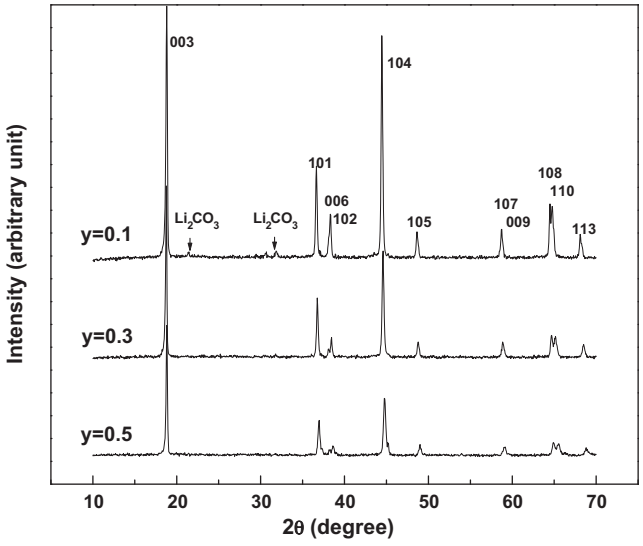

Fig. 2. XRD patterns of $LiNi_{1-y}Co_yO_2$ ($y = 0.1$, 0.3 and 0.5) powders calcined at 750 °C for 40 h from $LiOH{\cdot}H_2O$, NiO and Co_3O_4.

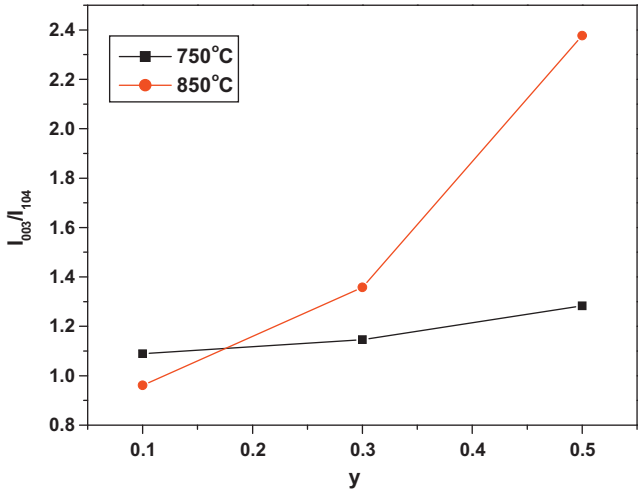

Fig. 4. Variation of intensity ratio of 0 0 3 and 1 0 4 peaks, $I_{0\,0\,3}/I_{1\,0\,4}$, with y in $LiNi_{1-y}Co_yO_2$ calcined at 750 °C and 850 °C for 40 h.

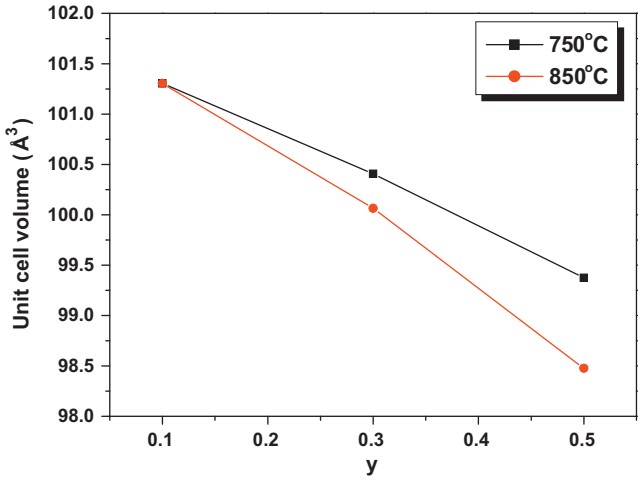

Fig. 5. Variation of unit cell volume with y in $LiNi_{1-y}Co_yO_2$ calcined at 750 °C and 850 °C.

temperature increases, the degree of displacement of the nickel and lithium ions decreases. The $I_{0\,0\,3}/I_{1\,0\,4}$ values of $LiNi_{0.7}Co_{0.3}O_2$ calcined at 850 °C and $LiNi_{0.5}Co_{0.5}O_2$ calcined at 850 °C are larger than 1.3, indicating that the composition of these samples is stoichiometric.

Dahn et al. [8] defined the intensity ratio, R, as the relative intensity of the (1 0 2, 0 0 6) Bragg peak near $2\theta = 38°$ as compared with that of the (1 0 1) peak near $2\theta = 36.5°$. Their results showed that the intensity ratio, R, increases as the unit cell volume increases. They also showed that the intensity ratio, R, increases rapidly as x decreases in $Li_xNi_{2-x}O_2$. This suggests that, as the unit cell volume increases, x decreases in $Li_xNi_{2-x}O_2$. $Li_xNi_{2-x}O_2$ can be expressed as $(Li_xNi_{1-x})NiO_2$. A decrease in x in $Li_xNi_{2-x}O_2$ corresponds to an increase in the degree of displacement of the nickel and lithium ions. The variations of unit cell volume with y in $LiNi_{1-y}Co_yO_2$ calcined at 750 °C and 850 °C for 40 h are given in Fig. 5. As the value of y increases, the unit cell volume decreases. This shows that as

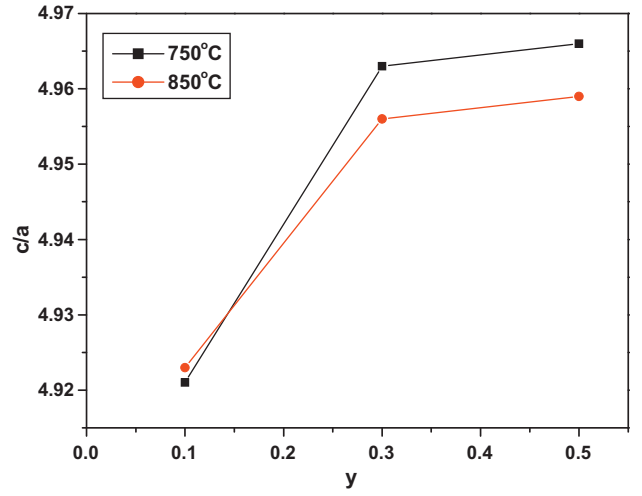

Fig. 6. Variation of the ratio c/a of lattice parameters a and c with y in $LiNi_{1-y}Co_yO_2$ synthesized at 750 °C and 850 °C for 40 h.

the Co content increases, the degree of displacement of the nickel and lithium ions decreases.

Variations of the degree of trigonal distortion, c/a, with y in $LiNi_{1-y}Co_yO_2$ calcined at 750 °C and 800 °C for 40 h are shown in Fig. 6. The value of c/a increases as y increases from 0.1 to 0.5. The increase in the value of c/a signifies a better development of two-dimensional structure.

The FE-SEM micrographs of $LiNi_{1-y}Co_yO_2$ ($y = 0.1$, 0.3 and 0.5) calcined at 750 °C for 40 h are presented in Fig. 7. The samples consist of small and large particles. The particle sizes increase slightly as the Co content increases. With increase in Co content the large particles become larger and the number of small particles decreases. It is known that $LiCoO_2$ can be easily prepared but stoichiometric $LiNiO_2$ is difficult to be obtained due to the similar sizes of Li and Ni [25,26]. As the Co content increases, it is considered that nucleation of the phase with the α-$NaFeO_2$ structure having a space group of $R\bar{3}m$ is facilitated, resulting in the increase in the overall growth rate of particles under the same period of calcination as the Co content increases.

Fig. 8 shows the FE-SEM micrographs of $LiNi_{1-y}Co_yO_2$ ($y = 0.1$, 0.3 and 0.5) calcined at 850 °C for 40 h. $LiNi_{0.7}Co_{0.3}O_2$ has a little smaller particles than $LiNi_{0.9}Co_{0.1}O_2$. The particle sizes of $LiNi_{0.5}Co_{0.5}O_2$ are much larger than $LiNi_{1-y}Co_yO_2$ ($y = 0.1$ and 0.3). The particles of $LiNi_{0.5}Co_{0.5}O_2$ have rounded shape. The particles of $LiNi_{0.9}Co_{0.1}O_2$ have the shape of polyhedron.

The particles of $LiNi_{1-y}Co_yO_2$ ($y = 0.1$, 0.3 and 0.5) calcined at 850 °C for 40 h (Fig. 8) are larger than those calcined at 750 °C for 40 h (Fig. 7).

The variations of discharge capacity at 200 μA/cm^2 with the number of cycles n for $LiNi_{1-y}Co_yO_2$ ($y = 0.1$, 0.3 and 0.5) calcined at 750 °C for 40 h are presented in Fig. 9. The sample $LiNi_{0.9}Co_{0.1}O_2$ has the largest first discharge capacity of 131.8 mAh/g, followed in order by $LiNi_{0.7}Co_{0.3}O_2$ (80.9 mAh/g) and $LiNi_{0.5}Co_{0.5}O_2$ (66.1 mAh/g). The sample $LiNi_{0.5}Co_{0.5}O_2$ has the best cycling performance with the discharge capacity of 42.6 mAh/g at $n = 10$, followed in order by $LiNi_{0.7}Co_{0.3}O_2$ and $LiNi_{0.9}Co_{0.1}O_2$. The discharge capacity fading rate of the sample $LiNi_{0.5}Co_{0.5}O_2$ is 2.7 mAh/g/cycle from $n = 1$ to $n = 10$. The sample $LiNi_{0.9}Co_{0.1}O_2$ has the discharge capacity of 72.1 mAh/g at $n = 10$, with the discharge capacity fading rate of 6.5 mAh/g/cycle from $n = 1$ to $n = 10$.

Fig. 10 shows the variations of discharge capacity at 200 μA/cm^2 with the number of cycles for $LiNi_{1-y}Co_yO_2$ ($y = 0.1$, 0.3 and 0.5) calcined at 850 °C for 40 h. The sample $LiNi_{0.7}Co_{0.3}O_2$ has the largest first discharge capacity of 146.2 mAh/g, followed in order by $LiNi_{0.5}Co_{0.5}O_2$ (134.4 mAh/g) and $LiNi_{0.9}Co_{0.1}O_2$ (113.3 mAh/g). The sample $LiNi_{0.7}Co_{0.3}O_2$ has the discharge capacity of 89.0 mAh/g at $n = 10$, with the discharge capacity fading rate of 6.3 mAh/g/cycle from $n = 1$ to $n = 10$.

Intercalation will cause expansion and deintercalation will cause contraction of the phase with the α-$NaFeO_2$ structure with a space group of $R\bar{3}m$. This will make the lattice strained and distorted. With cycling, the interstitial sites and thus the α-$NaFeO_2$ structure will be destroyed. This decreases the fraction

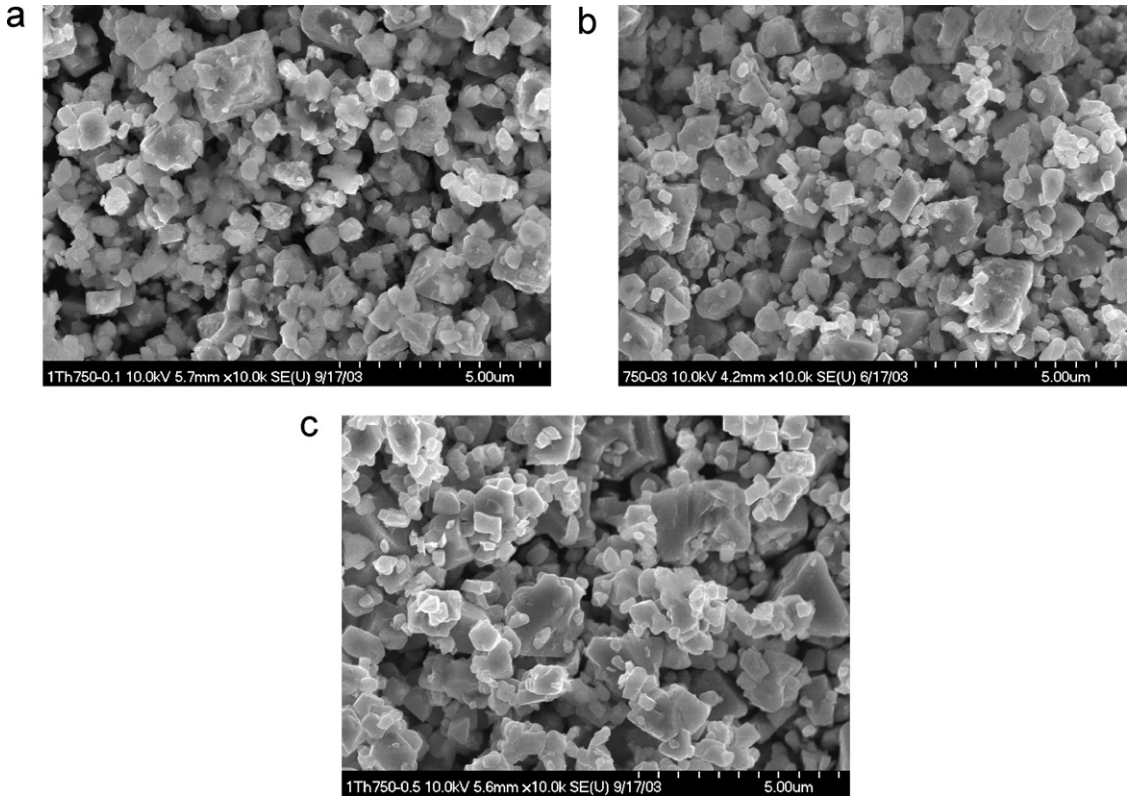

Fig. 7. FE-SEM micrographs of $LiNi_{1-y}Co_yO_2$ calcined at 750 °C for 40 h; (a) $y = 0.1$, (b) $y = 0.3$ and (c) $y = 0.5$.

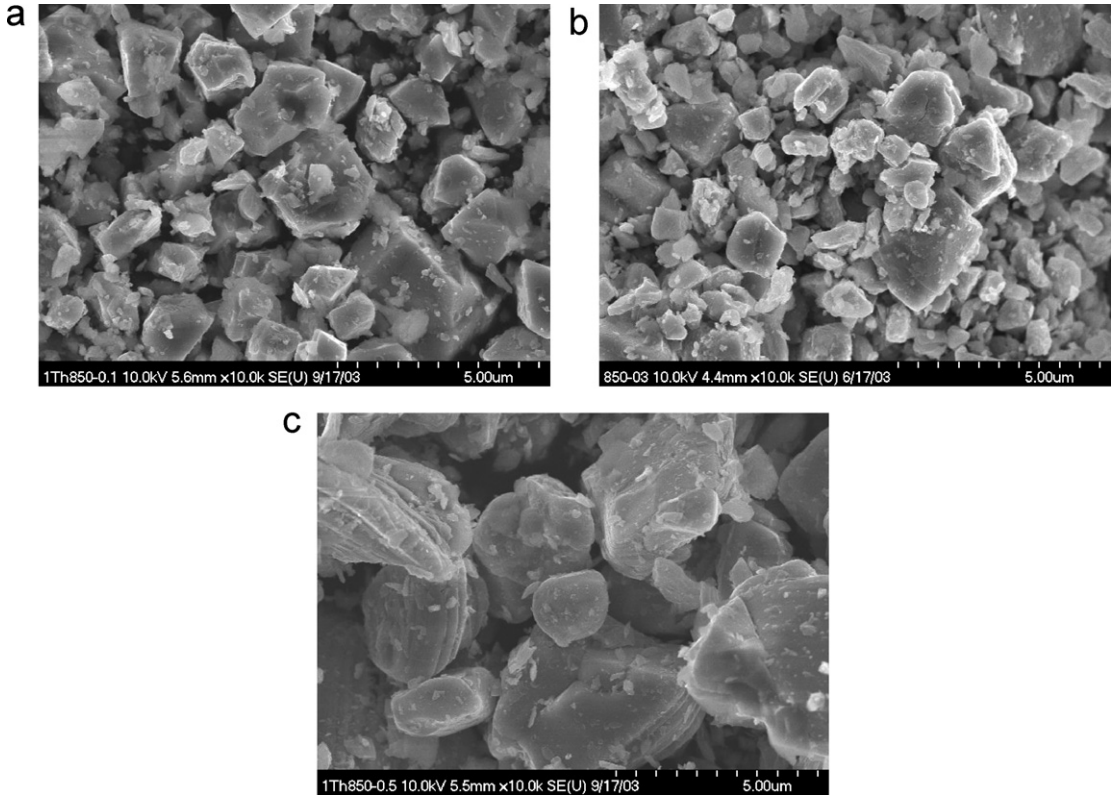

Fig. 8. FE-SEM micrographs of $LiNi_{1-y}Co_yO_2$ calcined at 850 °C for 40 h; (a) $y = 0.1$, (b) $y = 0.3$ and (c) $y = 0.5$.

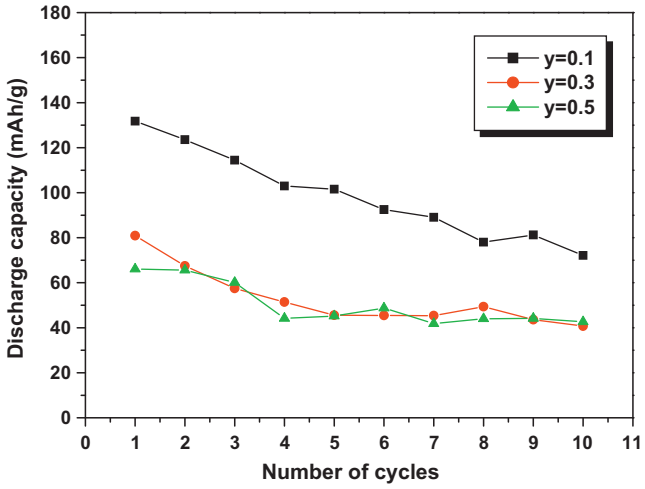

Fig. 9. Variations of discharge capacity at 200 μA/cm^2 with the number of cycles for $LiNi_{1-y}Co_yO_2$ calcined at 750 °C for 40 h.

of the α-$NaFeO_2$ structure phase, leading to the capacity fading of the sample with cycling.

The first discharge capacities of $Li_xCo_yNi_{1-y}O_2$, prepared by Kang et al. [42] under the conditions similar to those of this work, were 60–180 mAh/g depending on synthetic conditions. Among them, the $Li_xNi_{0.7}Co_{0.3}O_2$, which was prepared with LiOH, NiO, and Co_3O_4 at 850 °C, had the best electrochemical properties. The first discharge capacity of the compound was 180 mAh/g. The discharge capacities of $LiNi_{1-y}Co_yO_2$ prepared by Kang et al. [42] are larger than those of this work. This is believed because the samples of this work contain an impurity phase Li_2CO_3 even though its content decreases as the Co content and the calcination temperature increase.

Among all of the $LiNi_{1-y}Co_yO_2$ ($y = 0.1$, 0.3 and 0.5) samples calcined at 750 °C and 850 °C for 40 h, $LiNi_{0.7}Co_{0.3}O_2$ and $LiNi_{0.5}Co_{0.5}O_2$ calcined at 850 °C have relatively large first discharge capacities and relatively large discharge capacities. $LiNi_{0.7}Co_{0.3}O_2$ calcined at 850 °C has the largest first discharge capacity of 146.2 mAh/g, followed by $LiNi_{0.5}Co_{0.5}O_2$ calcined at 850 °C (134.4 mAh/g). $LiNi_{0.7}Co_{0.3}O_2$ calcined at 850 °C has a lower discharge capacity fading rate of 6.3 mAh/g/cycle than $LiNi_{0.5}Co_{0.5}O_2$ calcined at 850 °C (8.0 mAh/g/cycle). $LiNi_{0.7}Co_{0.3}O_2$ and $LiNi_{0.5}Co_{0.5}O_2$ calcined at 850 °C have relatively large values of $I_{0\,0\,3}/I_{1\,0\,4}$, and relatively small unit cell volumes, showing that the degree of displacement of the nickel and lithium ions is low in these samples. The low degree of displacement of the nickel and lithium ions in these samples is believed to result in their relatively large first discharge capacities and good cycling performances. These samples have relatively large values of c/a, signifying a better development of two-dimensional structure.

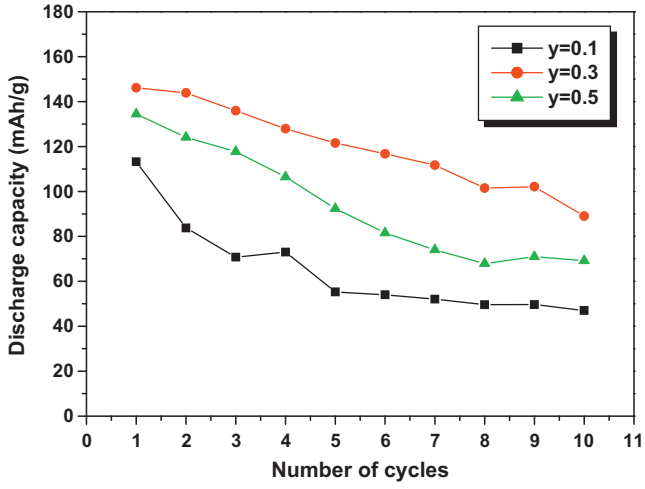

Fig. 10. Variations of discharge capacity at 200 μA/cm^2 with the number of cycles for $LiNi_{1-y}Co_yO_2$ calcined at 850 °C for 40 h.

4. Conclusions

$LiNi_{1-y}Co_yO_2$ ($y = 0.1$, 0.3 and 0.5) were synthesized by solid-state reaction method at 750 °C and 850 °C from $LiOH{\cdot}H_2O$, NiO and Co_3O_4. Among all of the $LiNi_{1-y}Co_yO_2$ ($y = 0.1$, 0.3 and 0.5) samples calcined at 750 °C and 850 °C for 40 h, $LiNi_{0.7}Co_{0.3}O_2$ and $LiNi_{0.5}Co_{0.5}O_2$ calcined at 850 °C have relatively large first discharge capacities and relatively large discharge capacities. $LiNi_{0.7}Co_{0.3}O_2$ calcined at 850 °C has the largest first discharge capacity of 146.2 mAh/g, followed by $LiNi_{0.5}Co_{0.5}O_2$ calcined at 850 °C (134.4 mAh/g). $LiNi_{0.7}Co_{0.3}O_2$ calcined at 850 °C has a lower discharge capacity fading rate of 6.3 mAh/g/cycle than $LiNi_{0.5}Co_{0.5}O_2$ calcined at 850 °C (8.0 mAh/g/cycle). $LiNi_{0.7}Co_{0.3}O_2$ and $LiNi_{0.5}Co_{0.5}O_2$ calcined at 850 °C have relatively large values of $I_{0\,0\,3}/I_{1\,0\,4}$, and relatively small unit cell volumes, showing that the degree of displacement of the nickel and lithium ions is low in these samples. These samples have relatively large values of c/a, signifying a better development of two-dimensional structure.

References

[1] K. Ozawa, Lithium-ion rechargeable batteries with $LiCoO_2$ and carbon electrodes: the $LiCoO_2$/C system, Solid State Ionics 69 (1994) 212–221.
[2] R. Alcántara, P. Lavela, J.L. Tirado, R. Stoyanova, E. Zhecheva, Structure and electrochemical properties of boron-doped $LiCoO_2$, J. Solid State Chem. 134 (1997) 265–273.
[3] Z.S. Peng, C.R. Wan, C.Y. Jiang, Synthesis by sol–gel process and characterization of $LiCoO_2$ cathode materials, J. Power Sources 72 (1998) 215–220.
[4] C.H. Han, J.H. Kim, S.H. Paeng, D.J. Kwak, Y.M. Sung, Electrochemical characteristics of $LiNiO_2$ films prepared for charge storable electrode application, Thin Solid Films 517 (14) (2009) 4215–4217.
[5] S.N. Kwon, J.H. Song, D.R. Mumm, Effects of cathode fabrication conditions and cycling on the electrochemical performance of $LiNiO_2$ synthesized by combustion and calcination, Ceram. Int. 37 (5) (2011) 1543–1548.
[6] J.M. Tarascon, E. Wang, F.K. Shokoohi, W.R. Mckinnon, S. Colson, The spinel phase of $LiMn_2O_4$ as a cathode in secondary lithium cells, J. Electrochem. Soc. 138 (1991) 2859–2864.
[7] A.R. Armstrong, P.G. Bruce, Synthesis of layered $LiMnO_2$ as an electrode for rechargeable lithium batteries, Lett. Nat. 381 (1996) 499–500.
[8] J.R. Dahn, U. von Sacken, C.A. Michal, Structure and electrochemistry of $Li_{1\pm y}NiO_2$ and a new Li_2NiO_2 phase with the $Ni(OH)_2$ structure, Solid State Ionics 44 (1990) 87–97.
[9] J.R. Dahn, U. von Sacken, M.W. Juzkow, H. Al-Janaby, Rechargeable $LiNiO_2$/carbon cells, J. Electrochem. Soc. 138 (1991) 2207–2212.

[10] Y. Kim, G.M. Veith, J. Nanda, R.R. Unocic, M. Chi, N.J. Dudney, High voltage stability of $LiCoO_2$ particles with a nano-scale Lipon coating, Electrochim. Acta 56 (19) (2011) 6573–6580.

[11] W.D. Yang, C.Y. Hsieh, H.J. Chuang, Y.S. Chen, Preparation and characterization of nanometric-sized $LiCoO_2$ cathode materials for lithium batteries by a novel sol–gel method, Ceram. Int. 36 (1) (2010) 135–140.

[12] H.U. Kim, D.R. Mumm, H.R. Park, M.Y. Song, Synthesis by a simple combustion method and electrochemical properties of $LiCo_{1/3}Ni_{1/3}Mn_{1/3}O_2$, Electron. Mater. Lett. 6 (3) (2010) 91–95.

[13] S.H. Ju, J.H. Kim, Y.C. Kang, Electrochemical properties of $LiNi_{0.8}Co_{0.2-x}Al_xO_2$ ($0 \leq x \leq 0.1$) cathode particles prepared by spray pyrolysis from the spray solutions with and without organic additives, Metals Mater. Int. 16 (2) (2010) 299–303.

[14] D.H. Kim, Y.U. Jeong, Crystal structures and electrochemical properties of $LiNi_{1-x}Mg_xO_2$ ($0 \leq x \leq 0.1$) for cathode materials of secondary lithium batteries, Korean J. Met. Mater. 48 (3) (2010) 262–267.

[15] M.Y. Song, D.R. Mumm, C.K. Park, H.R. Park, Cycling performances of $LiNi_{1-y}M_yO_2$ (M = Ni, Ga, Al and/or Ti) synthesized by wet milling and solid-state method, Metals Mater. Int., doi:10.1007/s12540-012-3013-3, in press.

[16] A. Marini, V. Massarotti, V. Berbenni, D. Capsoni, R. Riccardi, E. Antolini, B. Passalacqua, On the thermal stability and defect structure of the solid solution $Li_xNi_{1-x}O$, Solid State Ionics 45 (1991) 143–155.

[17] W. Ebner, D. Fouchard, L. Xie, The $LiNiO_2$/carbon lithium-ion battery, Solid State Ionics 69 (1994) 238–256.

[18] M.Y. Song, D.S. Ahn, On the capacity deterioration of spinel phase $LiMn_2O_4$ with cycling around 4 V, Solid State Ionics 112 (1998) 21–24.

[19] M.Y. Song, D.S. Ahn, H.R. Park, Capacity fading of spinel phase $LiMn_2O_4$ with cycling, J. Power Sources 83 (1999) 57–60.

[20] D.S. Ahn, M.Y. Song, Variations of the electrochemical properties of $LiMn_2O_4$ with synthesis conditions, J. Electrochem. Soc. 147 (3) (2000) 874–879.

[21] H.J. Guo, Q.H. Li, X.H. Li, Z.X. Wang, W.J. Peng, Novel synthesis of $LiMn_2O_4$ with large tap density by oxidation of manganese powder, Energy Convers. Manage. 52 (4) (2011) 2009–2014.

[22] C. Wan, M. Cheng, D. Wu, Synthesis of spherical spinel $LiMn_2O_4$ with commercial manganese carbonate, Powder Technol. 210 (1) (2011) 47–51.

[23] J.W. Park, J.H. Yu, K.W. Kim, H.S. Ryu, J.H. Ahn, C.S. Jin, K.H. Shin, Y.C. Kim, H.J. Ahn, Surface morphology changes of lithium/sulfur battery using multi-walled carbon nanotube added sulfur electrode during cyclings, Korean J. Met. Mater. 49 (2) (2011) 174–179.

[24] Y. Nishida, K. Nakane, T. Satoh, Synthesis and properties of gallium-doped $LiNiO_2$ as the cathode material for lithium secondary batteries, J. Power Sources 68 (1997) 561–564.

[25] P. Barboux, J.M. Tarascon, F.K. Shokoohi, The use of acetates as precursors for the low-temperature synthesis of $LiMn_2O_4$ and $LiCoO_2$ intercalation compounds, J. Solid State Chem. 94 (1991) 185–196.

[26] J. Morales, C. Perez-Vicente, J.L. Tirado, Cation distribution and chemical deintercalation of $Li_{1-x}Ni_{1+x}O_2$, Mater. Res. Bull. 25 (1990) 623–630.

[27] A. Rougier, I. Saadoune, P. Gravereau, P. Willmann, C. Delmas, Solid-State Ionics 90 (1996) 83–90.

[28] B.J. Neudecker, R.A. Zuhr, B.S. Kwak, J.B. Bates, J.D. Robertson, Lithium manganese nickel oxides $Li_x(Mn_yNi_{1-y})_{2-x}O_2$, J. Electrochem. Soc. 145 (1998) 4148–4157.

[29] C. Delmas, I. Saadoune, Electrochemical and physical properties of the $Li_xNi_{1-y}Co_yO_2$ phases, Solid-State Ionics 53–56 (1992) 370–375.

[30] E. Zhecheva, R. Stoyanova, Stabilization of the layered crystal structure of $LiNiO_2$ by Co-substitution, Solid-State Ionics 66 (1993) 143–149.

[31] C. Delmas, I. Saadoune, A. Rougier, The cycling properties of the $Li_xNi_{1-y}Co_yO_2$ electrode, J. Power Sources 43–44 (1993) 595–602.

[32] A. Ueda, T. Ohzuku, Solid-state redox reactions of $LiNi_{1/2}Co_{1/2}O_2$ ($R\bar{3}m$) for 4 volt secondary lithium cells, J. Electrochem. Soc. 141 (1994) 2010–2014.

[33] M. Menetrier, A. Rougier, C. Delmas, Cobalt segregation in the $LiNi_{1-y}Co_yO_2$ solid solution: a preliminary ^7Li NMR study, Solid State Commun. 90 (1994) 439–442.

[34] R. Alcantara, J. Morales, J.L. Tirado, R. Stoyanova, E. Zhecheva, Structure and electrochemical properties of $Li_{1-x}(Ni_yCo_{1-y})_{1+x}O_2$ effect of chemical delithiation at 0 °C, J. Electrochem. Soc. 142 (1995) 3997–4005.

[35] B. Banov, J. Bourilkov, M. Mladenov, Cobalt stabilized layered lithium–nickel oxides, cathodes in lithium rechargeable cells, J. Power Sources 54 (1995) 268–270.

[36] Y.M. Choi, S.I. Pyun, S.I. Moon, Effects of cation mixing on the electrochemical lithium intercalation reaction into porous $Li_{1-\delta}Ni_{1-y}Co_yO_2$ electrodes, Solid State Ionics 89 (1996) 43–52.

[37] S.J. Lee, J.K. Lee, D.W. Kim, H.K. Baik, S.M. Lee, Fabrication of thin film $LiCo_{0.5}Ni_{0.5}O_2$ cathode for Li rechargeable microbattery, J. Electrochem. Soc. 143 (1996) L268–L270.

[38] D. Caurant, N. Baffier, B. Garcia, J.P. Pereira-Ramos, Synthesis by a soft chemistry route and characterization of $LiNi_xCo_{1-x}O_2$ ($0 \leq x \leq 1$) cathode materials, Solid State Ionics 91 (1996) 45–54.

[39] K. Amine, H. Yasuda, Y. Fujita, New process for low temperature preparation of $LiNi_{1-x}Co_xO_2$ Cathode material for lithium cells, Ann. Chim. Sci. Mater. 23 (1998) 37–42.

[40] C.C. Chang, N. Scarr, P.N. Kumta, Synthesis and electrochemical characterization of $LiMO_2$ (M = Ni, $Ni_{0.75}Co_{0.25}$) for rechargeable lithium ion batteries, Solid State Ionics 112 (1998) 329–344.

[41] K. Kubo, S. Arai, S. Yamada, M. Kanda, Synthesis and charge–discharge properties of $Li_{1+x}Ni_{1-x-y}Co_yO_{2-z}F_z$, J. Power Sources 81–82 (1999) 599–603.

[42] S.G. Kang, K.S. Ryu, S.H. Chang, S.C. Park, The novel synthetic route to $LiCo_yNi_{1-y}O_2$ as a cathode material in lithium secondary batteries, Bull. Kor. Chem. Soc. 22 (12) (2001) 1328–1332.

[43] T. Ohzuku, A. Ueda, M. Nagayama, Electrochemistry and structural chemistry of $LiNiO_2$ ($R\bar{3}m$) for 4 volt secondary lithium cells, J. Electrochem. Soc. 140 (1993) 1862–1870.

[44] J. Morales, C. Pérez-Vicente, J.L. Tirado, Cation distribution and chemical deintercalation of $Li_{1-x}Ni_{1+x}O_2$, Mater. Res. Bull. 25 (1990) 623–630.